NATURAL RUBBER NANOCOMPOSITES WITH ORGANO-MODIFIED BENTONITE

Jana Hrachová[1],*, Peter Komadel[1], and Ivan Chodák[2]

[1] Institute of Inorganic Chemistry, Slovak Academy of Sciences, Dúbravská cesta 9, SK-845 36 Bratislava, Slovakia
[2] Polymer Institute, Slovak Academy of Sciences, Dúbravská cesta 9, SK-842 36 Bratislava, Slovakia

Abstract—Enhancement of the physico-chemical properties of elastomers can be achieved by the addition of fillers, such as silica, but the search for less expensive alternative materials continues. The objective of this study was to investigate natural or organically modified clay minerals as such an alternative. Organo-clays modified by quaternary ammonium cations with three methyl groups and longest alkyl chains of different lengths were prepared by ion-exchange reaction of the commercial product JP A030 (Envigeo, Slovakia) based on Jelšový Potok bentonite with organic salts: tetramethylammonium (TMA) chloride, octyltrimethylammonium (OTMA) bromide, and octadecyltrimethylammonium (ODTMA) bromide. Physico-chemical characterizations of the organo-clays used as fillers in rubber nanocomposites and their mechanical properties were measured using Fourier transform infrared (IR) spectroscopy, which provided information on the chemical composition of the mineral and on the amount of organic moieties adsorbed. X-ray diffraction analysis (XRD) was used to monitor the arrangement of organic chains in galleries of montmorillonite and showed that the longest-chain alkylammonium ODTMA$^+$ ions were intercalated between layers, adopting a pseudotrimolecular conformation, while OTMA$^+$ and TMA$^+$ were in monomolecular arrangement. Surface areas were measured by sorption of N_2 and ethylene glycol monoethyl ether. Natural rubber-clay nanocomposites were prepared by melt intercalation, in some cases also with addition of silica, a conventional reinforcing filler. The microstructure of montmorillonite in these composites was characterized by XRD analysis. The effect of clay and organo-clays loading from 1 to 10 phr (parts by weight per hundred parts of rubber) on stress at break, strain at break, and Modulus 100 (M100) was investigated by tensile tests. Filler ODTMA-JP A030 appears to be the most effective among the organoclays; surprisingly similar values of composite elongation and strength were obtained with unmodified bentonite JP A030.

Key Words—Clay, Layered Silicate, Mechanical Properties, Nanocomposite, Organo-clay, Polymer.

INTRODUCTION

The field of clay-based polymer nanocomposites has experienced enormous academic and industrial development due to their significantly modified properties in relation to conventional composites (micro/macrocomposites) or matrix alone (Okada and Usuki, 2006; Xue and Pinnavaia, 2007; Carrado and Komadel, 2009). Particulate fillers can be divided into two groups, inert fillers and reinforcing fillers. The former are added to the rubber to increase the bulk and reduce the costs. In contrast, reinforcing fillers such as carbon black, silica, or layered silicates are incorporated into the rubber to improve the mechanical and other properties (Arroyo *et al.*, 2003; Baccaro *et al.*, 2003; Ray and Bousmina, 2005; Liu *et al.*, 2008). The characteristic polymer-reinforcement properties of nanocomposites appear for layered silicate contents as small as 1−5 wt.% and the best effect is achieved when the individual clay layers are uniformly dispersed on a nanometer scale. Among these improvements, material stiffness increases while preserving remarkable toughness, and permeability to oxygen and some fluids is dramatically reduced com-

pared to pure polymers; thermal stability and fire retardancy are enhanced. Clay-based polymer nanocomposites can also exhibit interesting properties in terms of ionic conductivity or optical applications (Ray and Okamoto, 2003; Pavlidou and Papaspyrides, 2008).

Montmorillonite is currently the most widely used clay mineral nanofiller because of its cation-exchange capacity and large active surface area when sufficiently delaminated. The layer thickness is ~1 nm, while the lateral dimensions of the layers vary up to several microns or even more, *i.e.* at least one dimension is in the nanometer range. Of particular interest is recently developed nanocomposite technology consisting of interactions of a polymer and organically modified smectite (organo-clay) (Cataldo, 2007; Gao *et al.*, 2008; Hrachová *et al.*, 2008). When hydrophilic inorganic exchangeable Ca^{2+} or Na^+ is replaced by organic cations such as alkylammonium cations, the clay mineral surfaces become more hydrophobic resulting in an improved compatibility with polymers. Alkylammonium or alkylphosphonium cations in the organo-clays lead to a decrease of the surface energy of the inorganic host and improve the wetting of the filler surface by polymer matrix, resulting in larger interlayer spacing. The aforementioned cations can provide functional groups that may react with the polymer matrix, or even initiate the polymerization of monomers to improve

* E-mail address of corresponding author:
Jana.Hrachova@savba.sk

interactions on the interface between the inorganic and the polymer matrix (Krishnamoorti *et al.*, 1996).

A range of different composite structures: separate-phase (microcomposite), intercalated, exfoliated, and mixed intercalated/exfoliated nanocomposite can be obtained, depending on the degree of penetration of the polymer chains into the silicate galleries (Alexandre and Dubois, 2000; Tjong, 2006). Although clay nanocomposites have been prepared and tested for many thermoplastic and thermosetting polymers, much less attention has been devoted to the elastomer-clay nanocomposites. Elastomers are generally hydrocarbon-based polymers consisting of carbon and hydrogen atoms, and include styrene-butadiene rubber, butyl rubber, polybutadiene rubber, ethylene propylene rubber, and polyisoprene-rubber, both natural and synthetic. Natural rubber (NR) is a linear polymer consisting of isoprene units (C_5H_8) and containing small amounts of fatty acids and proteinaceous residues, which may promote curing of sulfur (Mohammad and Simon, 2006). Important commercial applications of NR are in the production of tires, bumpers, and thin-walled, high-strength products such as balloons and surgical gloves. The favored means of preparing the rubber-clay nanocomposite consists of direct melt intercalation, when the smectites are mixed with the polymer matrix in the molten state. Depending on the mixing conditions and clay-layer surface compatibility with the polymer, the polymer chains can form either intercalated (with substantially expanded interlayers by the polymer and parallel layers) or exfoliated morphologies (with large separation of the layers and no layer stacking shown by XRD) (Dubois, 2007).

The objective of this study was to prepare and characterize nanocomposites of natural rubber and a commercial bentonite product with or without modification by one of three organic cations. Nanocomposites here mean clay-polymer materials containing smectite with dominantly delaminanted or exfoliated layers.

EXPERIMENTAL

Clay and organo-clays

The clay used in this study was Jelšový Potok A030 (JP A030), a bentonitic industrial non-activated product (Envigeo Inc., Slovakia). This material is a natural, processed bentonite with primarily Ca and Mg as exchanged cations. Its chemical composition given in wt.% is 65.29% SiO_2, 17.84% Al_2O_3; 2.25% Fe_2O_3, 3.44% MgO, 1.58% CaO; 1.45% K_2O; 0.82% Na_2O, loss in ignition 6.58%. The cation exchange capacity (CEC) is 69 meq/100 g. The main mineral is montmorillonite (>50%); quartz dominates among the accessory minerals. Three readily available surfactants with different-length alkylammonium chains were used for ion-exchange of the starting clay: tetramethylammonium (TMA) chloride (≥98%, Fluka), octyltrimethylammonium (OTMA) bromide (≥98%, Fluka), and octadecyl-

trimethylammonium (ODTMA) bromide (≥97%, Aldrich), in the preparation of organo-clays TMA-JP A030, OTMA-JP A030, and ODTMA-JP A030, respectively. The method of clay modification was very similar for all the surfactants. Solutions of appropriate concentrations were obtained by dissolving the organic salts in the required amount of a 1:1 mixture of water and ethanol heated to 60ºC. The amount of alkylammonium cations used was twice the CEC for $ODTMA^+$ and $OTMA^+$ and five times the CEC for TMA^+ cations to ensure complete exchange. The TMA^+ appears to have high selectivity in displacing inorganic exchangeable Mg^{2+}, but less than that of long-chain alkylammonium cations, *e.g.* HDTMA (Boyd and Jaynes, 1993). The solid/liquid ratio was 1 g of montmorillonite in 100 mL of the sorbate solution. The clay was dispersed carefully in deionized water using a magnetic stirrer at 60ºC and the organic solution was added slowly to the clay suspension under agitation. The reaction mixture was stirred intensively for 2 h (TMA-JP A030 for 24 h) at 60ºC and left to stand at room temperature for 24 h; after decantation the solution was replaced with fresh organic solution. The white precipitate formed was isolated by filtration and the excess bromide or chloride and organic ions in the organo-clay were removed by repeated washing with a mixture of hot water and ethanol (50/50) until a negative result of the $AgNO_3$ test was obtained. The sample was dried in air, first at room temperature and then at 50ºC, and then ground to particles of <200 μm diameter.

Characterization of clays

The organic content of the samples was estimated by CHN elemental analysis using an EA 1108 instrument.

The powder XRD profiles for compressed powder samples were recorded on a STOE STADI-P diffractometer, using CoKα radiation.

The infrared spectra were recorded using a Nicolet Magna 750 FTIR spectrometer equipped with a DTGS detector in the $4000-400$ cm^{-1} spectral range with a resolution of 4 cm^{-1}. The KBr pressed disc technique (1.0 mg sample and 200 mg KBr) was used: the KBr discs were heated in a furnace overnight at 130ºC to minimize the amount of adsorbed water in KBr and in the clays. All spectral manipulations were performed using the *OMNIC* software package (Nicolet Instruments Corp.).

The total specific surface areas of clays and organo-clays were determined by ethylene glycol monoethyl ether (EGME) adsorption. The samples were dried under vacuum in a desiccator over P_2O_5 for 48 h and then weighed. A few drops of EGME were added to each sample and the samples were stored under vacuum in a desiccator over ignited $CaCl_2$. They were weighed every 90 min until constant mass was achieved and the total specific surface area was then calculated according to Novák and Čičel (1972).

The BET surface area measurements were performed using an automated nitrogen adsorption apparatus (ASAP2400, Micromeritics). Prior to adsorption, the samples were degassed in a vacuum at 120ºC for 12 h. Relative pressures (p/p_0) between 0.05 and 0.30 were applied for the calculation of BET-N_2 surface areas.

Preparation of rubber-clay nanocomposites

Natural rubber SMR-20 (NR; Malaysia) was used as the elastomeric matrix and Silica Ultrasil VN3 (Evonik Industries, Germany) as the conventional reinforcement filler, commonly used in the rubber industry. The blends were prepared by mixing natural rubber with the filler and all the vulcanization ingredients except sulfur (Natural rubber (100 phr), clay (0−10 phr), silica (0 or 15 phr), zinc oxide (5 phr), stearic acid (2 phr), Sulfenax CBS/MG (3.5 phr), and sulfur (3.5 phr)) in a 50 mL mixing chamber of a Brabender Plasti-Corder PLE 331 at 70ºC for 14 min at the mixing speed 30 rpm. Composites with four different amounts of organo-clay fillers, 1, 3, 5, and 10 phr (parts by weight per hundred parts of rubber), were compounded. A comparative set of composites with the corresponding unmodified JP A030 was also prepared. Sulfur was added in a separate, second step on a roll mill. Slabs were obtained by compression molding of the mixed composite using a laboratory press Fontijne 200 (Fontijne, The Netherlands) at 150ºC for 35 min (optimum vulcanization time determined by rheometry) under 22.5 kN cm^{-2}. Seven dumbbel specimens with a working area of 35 mm × 3.6 mm × 1 mm were cut mechanically from each vulcanized slab.

Characterization of nanocomposites

The mechanical properties were measured at room temperature using an Instron 4301 universal testing machine at a deformation rate (crosshead speed) of 50 mm/min. Tensile strength, elongation at break, and Modulus at 100% elongation (M100) were determined. All measurements were made on 5−7 dumbbell specimens for each sample and the values were averaged.

The XRD profiles for composites containing 3 phr of the filler were recorded using a Bruker D8 Discover diffractometer (CuKα radiation, 40 kV/300 mA).

RESULTS AND DISCUSSION

Characterization of the clay and organo-clays

The XRD patterns in the 3−10º2θ region provided information on the cations present in the interlayers of montmorillonite (Figure 1). Although the parent material JP A030 was produced from non-activated bentonites selectively extracted and processed, it was not a homo-ionic form, containing mainly but not exclusively hydrated Ca^{2+} cations. The trace of JP A030 exhibited an intense symmetric diffraction with $d_{001} = 1.49$ nm, a value typical for montmorillonite with Ca^{2+} exchange-

able cations. Two parameters define the equilibrium basal spacing of the organo-clays: the cation exchange capacity of montmorillonite and the size of the organic cation, dominated by the length of the longest alkyl chain. The orientation of the intercalated alkyl chain depends on the layer-surface charge density. As shown in Figure 1, the d_{001} spacing of organo-clays and their hydrophobicity increased with the chain length of the organic cations and the shape of the diffraction peak changed also. The symmetric profile in the XRD pattern of the TMA$^+$-form indicated a similar arrangement of the cations in the interlayers of this sample. The d_{001} value of 1.39 nm was slightly less than that of JP A030 because of the small TMA$^+$ size and lesser hydration than that of Ca^{2+}. Much less symmetric and broader diffraction obtained for OTMA-JP A030 proved a more irregular arrangement of the species in its interlayers, some of the layers being more distant than the maximum 1.42 nm would suggest. Some of the octyl chains may occur in an arrangement more complex than monomolecular. The d_{001} value of ODTMA-JP A030 of 2.09 nm suggests a successive exchange of inorganic cations in the original material by substantially larger ODTMA$^+$ cations. The long-chain alkylammonium ions were intercalated between the layers during the cation-exchange process adopting a pseudotrimolecular arrangement; a layer consisting of three alkyl chains in which the non-polar chain ends were shifted one above the other by the formation of kinks (Mermut and Lagaly, 2001) of different sizes causing variation in the d_{001} value around 2.09 nm. Increased interlayer spacing as well as greater hydrophobicity of the organo-clays is essential for the polymer molecules to intercalate this type of filler.

The FTIR spectra of the clay fillers (Figure 2) revealed a broad band near 3430 cm^{-1}, observed more
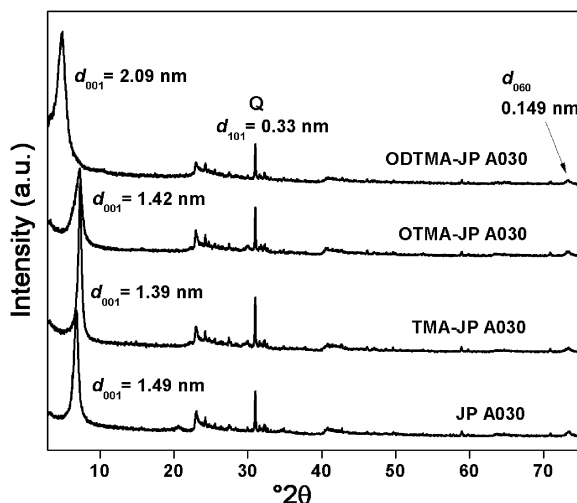

Figure 1. XRD patterns of the clay and organo-clay fillers investigated. Only the most intense diffraction of the quartz (Q) admixture is identified.
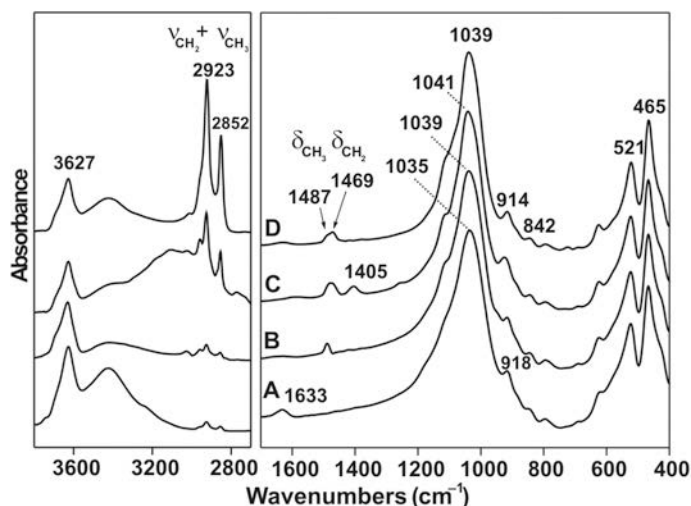
Figure 2. FTIR spectra of clay and organo-clays in the $3800-2700$ cm^{-1} and $1700-400$ cm^{-1} regions: JP A030 (A), TMA-JP A030 (B), OTMA-JP A030 (C), ODTMA-JP A030 (D).

or less clearly in the spectra of all materials, which is due to H-O-H vibrations of the adsorbed water. The intensity of this band is clearly greatest in the spectrum of the parent clay JP A030 (Figure 2A), which is naturally hydrophilic. The band near 1600 cm^{-1} is the most intense in the same spectrum. This confirms that the natural clay contains the most water. Much less absorption in both of these regions was also observed in the spectra of all organo-clays showing the presence of some water in the measured discs. The C-H stretching bands of alkylammonium cations occur in the $3020-2800$ cm^{-1} region (Madejová, 2003). Two strong narrow bands at 2922 cm^{-1} and 2850 cm^{-1} due to the asymmetric and symmetric (CH$_2$) vibrations, respectively, are present in the spectra of samples OTMA-JP and ODTMA-JP (Figure 2C,D). However, no clearly resolved stretching band appeared in the TMA-JP spectrum (Figure 2B). A characteristic asymmetric (C-H) bending vibration of the (CH$_3$)$_4$N$^+$ cation at 1487 cm^{-1} was seen in the spectrum of TMA-JP (Figure 2B). Replacement of one methyl group in (CH$_3$)$_4$N$^+$ with a longer alkyl chain (CH$_3$)$_3$N$^+$(CH$_2$)nCH$_3$ gives two strong bands near 1488 and 1469 cm^{-1} attributed to the asymmetric (C-H) bending vibration of both CH$_3$ and CH$_2$ groups. As a result of replacing the inorganic with organic cations, the clay surface takes on an hydrophobic nature, which makes it compatible with the hydrophobic polymer matrix and substantially improves the clay dispersion in the polymer.

Features observed in the XRD patterns and FTIR spectra are in accordance with the increasing amount of organic species as determined by the CHN analyses. The amounts of TMA$^+$, OTMA$^+$, and ODTMA$^+$ cations adsorbed on JP A030 represent 0.55, 0.72, and 1.20 mmol/g, respectively, corresponding to 80, 104, and 174% of the CEC (0.69 mmol/g), respectively. The

specific surface areas (SSAs) of the samples and commercial silicas investigated are presented (Table 1). The effect of surface modification with organic cations on the sorption of EGME and BET-N$_2$ must be taken into consideration in order to interpret the data correctly. The EGME SSA represents the total SSA, including the external surfaces of the particles and internal surfaces of the interlayers. The value of 569 m^2 measured for JP A030 is less than obtained for the montmorillonites separated from this bentonite ($\sim$ 800 m^2) (Hrachová et al., 2009), in accordance with the smaller amount of montmorillonite in JP A030. The total specific surface area for all the organo-clays was similar (205, 211, and 233 m^2), increasing slightly with shorter-length alkylammonium chains and showing no significant difference in the availability of these materials for sorption of ethylene glycol monoethyl ether species. The BET-N$_2$ SAs of the samples containing long alkylammonium cations were rather small, 5 and 28 m^2 for ODTMA- and OTMA-JP A030,

Table 1. BET and EGME specific surface areas of the investigated samples and two commercial silicas commonly used as reinforcement fillers in the rubber industry.

Material	Specific surface area (m^2)	
	BET	EGME
JP A030	28.1	569
TMA-JP A030	124	233
OTMA-JP A030	16.8	211
ODTMA-JP A030	5.1	205
Ultrasil VN3	130–200*	131
Ultrasil 7000	175*	236

*data from the producer (Evonik Industries)

respectively; however, an SA value for TMA-JP A030 of 124 m^2 was even greater than that for the parent JP-A030. The TMA-smectites had BET-N$_2$ surface areas of 100−200 m^2 (Boyd and Jaynes, 1993), a possible consequence of different coverage of the surface by much smaller TMA$^+$ cations compared to larger OTMA$^+$ or ODTMA$^+$ species, enabling increased adsorption of nitrogen molecules on the TMA-JP A030 surface. The results are in accordance with the data of Zhu *et al.* (2008). The surface areas of organo-clays with relatively large surfactant loadings, as calculated from CHN analysis results, were extremely small.

Nanocomposite properties and structural characterization

The mechanical properties (strain at break, stress at break, and Modulus 100) for NR composites in relation to the amount of filler (in the range 0−10 phr) are shown in Figures 3 and 4. The tensile properties (strain and stress at break) of all composites increased with increasing amount of fillers in all cases; the fillers differ in terms of their influence on mechanical properties, however (Figure 3a,b). The reinforcing effect, due to the presence of organo-modified fillers, increased with the increasing length of the alkyl chains in the alkylammonium cation; the same effect was observed for both tensile strength and elongation at break (Figure 3a,b). Surprisingly, the reinforcement achieved with unmodified filler was close to that for the most effective organo-modifier and clearly outperformed the modified fillers with shorter alkyl chains. This corresponds to the inter-gallery distance for the fillers (Figure 1), where the distance for ODTMA-JP A030 was larger while the distance for the other two organo-clays was very similar to that found for JP A030. Although the XRD data shown in Figures 5 and 6, for the fillers mixed in the NR matrix, present somewhat different results, a certain amount of intercalation must have occurred for the filler modified with the largest organic cation.

Besides composites with varying amounts of clays, composites with combinations of clay and 15 phr of common, highly reinforcing filler silica, Ultrasil VN3, were investigated (Figure 4a−c). Significant reinforcement is achieved with the addition of silica. The effect of adding 15 phr of silica was more or less the same as that of adding 10 phr of the two most effective fillers, JP A030 and ODTMA-JP A030. Addition of bentonite, either unmodified or organo-modified, to the mixture of NR with silica should lead to a substantially improved reinforcement, with 3 wt.% of the filler. In this case, any organic modification results in a decrease in the reinforcing effect.

The reinforcing effect was also estimated in terms of Modulus 100 (M100), a parameter used widely in rubber technology; Modulus 100 is the level of stress needed to achieve elongation of 100% (Figures 3c, 4c). The
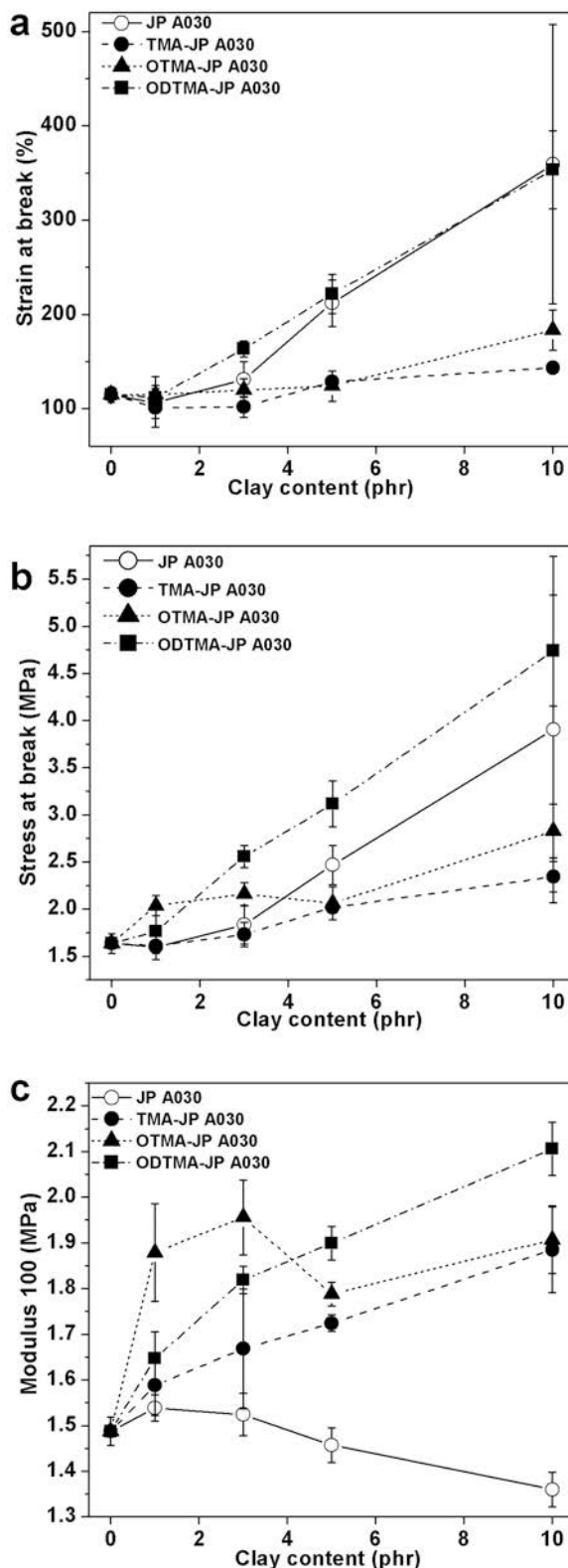

Figure 3. Mechanical properties of the nanocomposites of NR rubber in relation to the amount of clay (JP A030) and organo-clays (TMA-JP A030, OTMA-JP A030, and ODTMA-JP A030): strain at break (a), stress at break (b), and Modulus 100 (c).
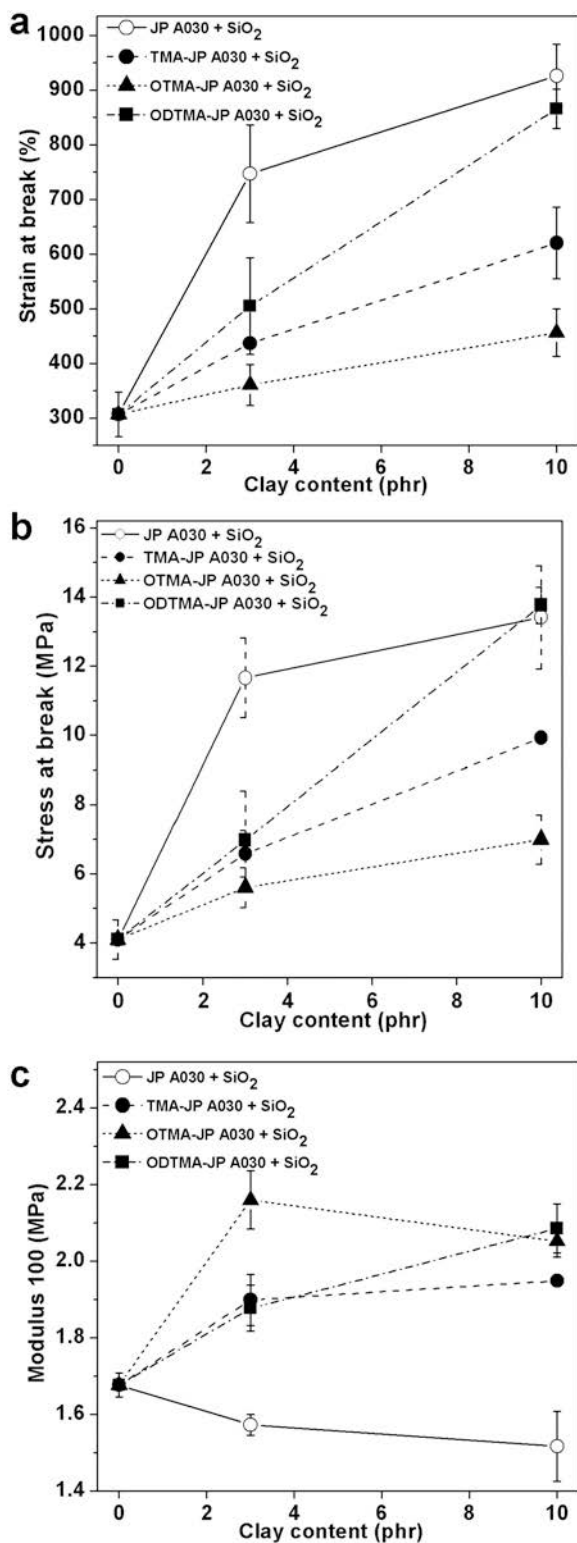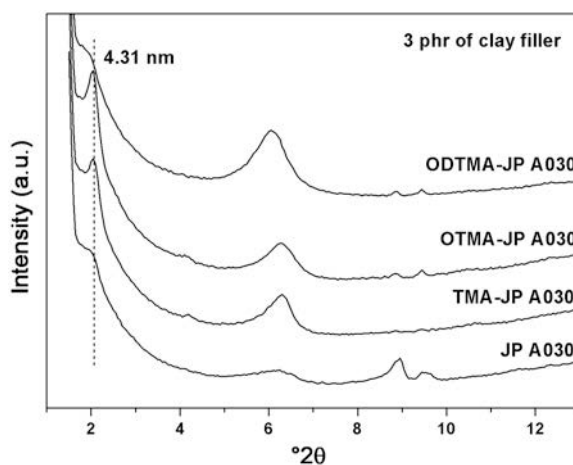
Figure 5. XRD patterns of nanocomposites of NR rubber with 3 phr of JP A030, TMA-JP A030, OTMA-JP A030, and ODTMA-JP A030.

behaviors of the three modified fillers and of the unmodified filler were different. While the addition of organo-clays resulted in an increase in the M100, a decrease of this parameter was observed after addition of JP A030. As the M100 values are roughly related to the network density, the modified fillers may form a type of very loose physical network influencing the mechanical properties at low deformation. The network decays at deformation of ~100% so that it is no longer effective. The formation of this network may have been a result of interactions between the surfaces of individual particles or between the filler surface and the matrix. As the organic modification should have led to improved compatibility between filler surface and the matrix, the latter suggestion is preferred, in full agreement with the stresses necessary to achieve a greater degree of deformation. Although the scatter of the results was

Figure 4. Mechanical properties of the nanocomposites of NR rubber with 15 phr of silica in relation to the amount of clay (JP A030) and organo-clays (TMA-JP A030, OTMA-JP A030, and ODTMA-JP A030): strain at break (a), stress at break (b), and Modulus 100 (c).
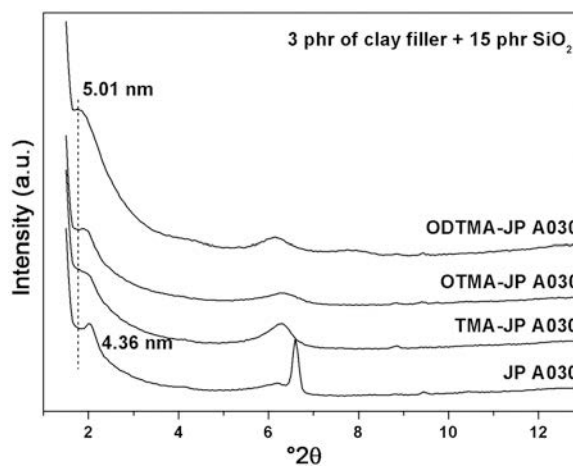

Figure 6. XRD patterns of nanocomposites of NR rubber with 15 phr of silica and 3 phr JP A030, TMA-JP A030, OTMA-JP A030, and ODTMA-JP A030.

greater than that for tensile strength and deformation, the general trend of the effect of the length of organic cation can be considered as supported also by results for M100. For unmodified JP A030, with and without silica, a decrease in the M100 parameter was observed with increasing clay content, as is commonly the case for reinforcing fillers, and indicates the lesser strength of composites during initial deformation. The organo-clays are able to act as reinforcing fillers due to their high aspect ratio and platelet structure. Loading of 1 and 3 phr of OTMA-JP A030 led to significant increase in M100 values for composites without silica, which surpassed the values obtained for the composite with 5 phr of ODTMA-JP A030 or with 10 phr ODTMA-JP in the presence of silica. The reinforcing effect declined with larger amounts of OTMA-JP A030 (5 or 10 phr). For the TMA-JP A030 filler, the correlation between stress and strain at break was almost linear Figures 7, 8) and the composite load of 10 phr of TMA-JP A030 achieved ~88% of the M100 value for the ODTMA-JP A030 composite (Figures 3c, 4c). Similar trends of M100 were observed for composites with 15 phr of silica and for composites without silica.

Under deformation of natural rubber, an effect of rubber crystallization under stress was observed: as ultimate deformation at break increases, tensile strength also increases. Obtaining high stress at break with a small deformation at break is, therefore, impossible. Furthermore, comparison of the dependence of stress at break on strain at break (Figures 7 and 8) indicates possible differences in deformation mechanisms of the various natural rubber-based materials, even though all three reinforcing fillers gave identical stress-strain relationships. For rubber filled with unmodified bentonite, on the other hand, less stress was needed to achieve the same deformation. A certain amount of reinforcement is imparted by organo-modification; fillers do not affect the crystallization of the rubber during deformation. The addition of silica leads to a unification of the

effect so that the stress-strain dependencies for all the fillers are the same. The deformation mechanism of all the fillers investigated is the same; the fillers differ in terms of the strength of their physical interactions (filler-filler or matrix-filler) on the phase boundaries, resulting in different mechanical properties.

X-ray diffraction is used widely to probe the fillers in nanocomposites. Information on the state of the filler can be obtained from the position, shape, and intensity of the basal (001) diffraction of montmorillonite. In comparison with the spacing in the organo-clays used, the intercalation of polymer chains leads to an increase in the interlayer spacing; attractive forces between the cations and the layers, however, may be strong enough to stack them into an ordered structure. In contrast, in exfoliated structures no (001) diffraction peaks appear in the patterns (Tjong, 2006; Pavlidou and Papaspyrides, 2008). The XRD traces of rubber-clay nanocomposites with 3 phr of clay filler (Figures 5 and 6) revealed significantly larger interlayer distances for both types of rubber-clay mixtures in comparison with neat organo-clays (Figure 1). Well defined (001) diffraction peaks appeared for composites without silica and with TMA- or OTMA-JP A030 fillers (Figure 5), while the (001) diffraction in the ODTMA-JP A030 was much broader. In the presence of silica (Figure 6), the (001) diffraction peaks were clearly visible in the patterns of composites with all fillers; the largest interlayer distance was achieved with ODTMA-JP A030. The presence of silica in the composites led to better dispersion of the filler and, as a result, to improvement of the mechanical properties due to the greater viscosity of the rubber matrix, indicating the possible formation of nanocomposites with intercalated and/or partially exfoliated structure of montmorillonite.

CONCLUSIONS

Natural rubber-clay nanocomposites were prepared *via* melt intercalation with bentonite or organically
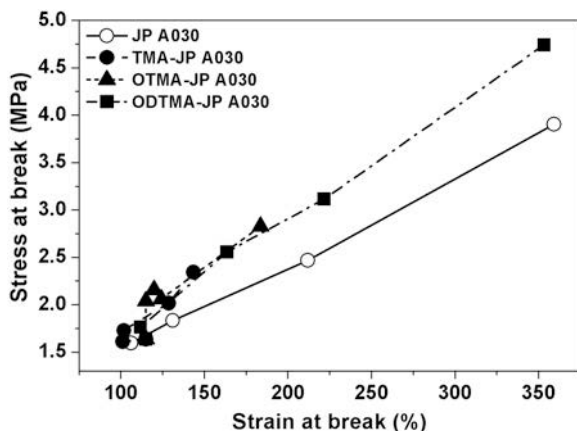

Figure 7. Tensile strength *vs.* deformation at break in rubber-clay nanocomposites.
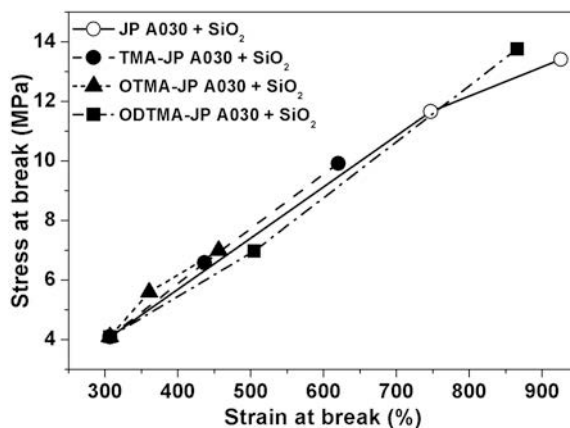

Figure 8. Tensile strength *vs.* deformation at break in rubber-clay nanocomposites with 15 phr silica.

modified clays used as fillers. Mechanical properties of natural rubber with or without silica were enhanced by addition of clay fillers. Similar values of composite elongation and of composite strength were obtained for materials with ODTMA-JP A030 or unmodified JP A030 and also for both materials with silica. Organoclays with shorter alkyl chains were less effective. The greatest elongation values of all composites with silica were obtained for those containing JP A030. The addition of silica led to enhancement of the mechanical properties of the composite with small TMA^+ cations. Addition of 10 phr of JP A030 resulted in an increase in the strain of the composites by 52% compared with that containing 15 phr of silica, while the stress values were similar. This result is promising for possible substitution of more expensive silica with unmodified clay in natural rubber nanocomposites. The formation of intercalated or partially exfoliated nanocomposites occurred. Greater interlayer distances were observed for composites with silica, possibly because of the greater viscosity of the rubber matrices which also contained silica as filler.

ACKNOWLEDGMENTS

REFERENCES

Alexandre, M. and Dubois, P. (2000) Polymer-layered silicate nanocomposites: preparation, properties and uses of a new class of materials. *Materials Science and Engineering*, **R28**, 1–63.

Arroyo, M., López-Manchado, M.A., and Herrero, B. (2003) Organo-montmorillonite as substitute of carbon black in natural rubber compounds. *Polymer*, **44**, 2447–2453.

Baccaro, S., Cataldo, F., Cecilia, A., Cemmi, A., Padella, F., and Santini, A. (2003) Interaction between reinforced carbon black and polymeric matrix for industrial applications. *Nuclear Instruments and Methods in Physics Research*, **B208**, 191–194.

Boyd, S.A. and Jaynes, W.F. (1993) Role of layer charge in organic contaminant sorption by organo-clays. Pp. 47–78 in: *Layer Charge Characteristics of 2:1 Silicate Clay Minerals* (A.R. Mermut, editor). CMS Workshop Lectures, Vol. **6**, The Clay Minerals Society, Boulder, Colorado, USA.

Dubois, P. (2007) Melt-blending versus intercalative polymerization. Pp. 33–60 in *Clay-based Polymer Nanocomposites (CPN)* (K.A. Carrado and F. Bergaya, editors). CMS workshop lectures, **15**, The Clay Minerals Society, Chantilly, VA, USA.

Carrado, K.A. and Komadel, P. (2009) Acid activation of bentonites and polymer-clay nanocomposites. *Elements*, **5**, 111–116.

Cataldo, F. (2007) Preparation and properties of nanostructured rubber composites with montmorillonite. *Macromolecular Symposia*, **247**, 67–77.

Gao, J., Gu, Z., Song, G., Li, P., and Liu, W. (2008) Preparation and properties of organo-montmorillonite/fluoroelastomer nanocompposites. *Applied Clay Science*, **42**, 272–275.

Hrachová, J., Komadel, P., and Chodák, I. (2008) Effect of montmorillonite modification on mechanical properties of vulcanized natural rubber composites. *Journal of Materials Science*, **43**, 2012–2017.

Hrachová, J., Chodák, I., and Komadel, P. (2009) Modification and characterization of montmorillonite fillers used in composites with vulcanized natural rubber. *Chemical Papers*, **63**, 55–61.

Krishnamoorti, R., Vaia, R.A., and Giannelis, E.P. (1996) Structure and dynamics of polymer layered silicate nanocomposites. *Chemical Materials*, **8**, 1728–1734.

Liu, Q., Zhang, Y., and Xu, H. (2008) Properties of vulcanized rubber nanocomposites filled with nanokaolin and precipitated silica. *Applied Clay Science*, **42**, 232–237.

Madejová, J. (2003) FTIR techniques in clay mineral studies. *Vibrational Spectroscopy*, **31**, 1–10.

Mermut, A.R. and Lagaly, G. (2001) Baseline studies of The Clay Minerals Society Source Clays: Layer-charge determination and characteristics of those minerals containing 2:1 layers. *Clays and Clay Minerals*, **49**, 393–397.

Mohammad, A. and Simon, G.P. (2006) Rubber-clay nanocomposites. Pp. 297–325 in *Polymer Nanocomposites* (Yiu-Wing Mai and Zhong-Zhen Yu, editors). Woodhead Publishing Limited, Cambridge, England.

Novák, I. and Číčel, B. (1972) Refinement of surface area determining of clays by ethylene glycol monoethyl ether (EGME) retention. Pp. 123–129 in: *Proceedings of the Fifth Conference on Clay Mineralogy and Petrology* (J. Konta, editor). Charles University, Prague.

Okada, A. and Usuki, A. (2006) Twenty years of polymer-clay nanocomposites. *Macromolecular Materials and Engineering*, **291**, 1449–1476.

Pavlidou, S. and Papaspyrides, C.D. (2008) A review on polymer-layered silicate nanocomposites. *Progress in Polymer Science*, **33**, 1119–1198.

Ray, S.S. and Bousmina, M. (2005) Biodegradable polymers and their layered silicate nanocomposites: In greening the 21st century materials world. *Progress in Materials Science*, **50**, 962–1079.

Ray, S.S. and Okamoto, M. (2003) Polymer/layered silicate nanocomposites: a review from preparation to processing. *Progress in Polymer Science*, **28**, 1539–1641.

Tjong, S.C. (2006) Structural and mechanical properties of polymer nanocomposites. *Materials Science and Engineering*, **R53**, 73–197.

Xue, S. and Pinnavaia, T.J. (2007) Overview of clay-based polymer nanocomposites (CPN). Pp. 2–32 in: *Clay-based Polymer Nanocomposites (CPN)* (K.A. Carrado and F. Bergaya, editors). CMS workshop lectures, vol. **15**, The Clay Minerals Society, Chantilly, VA, USA.

Zhu, R., Zhu, L., Zhu, J., and Xu, L. (2008) Structure of surfactant-clay complexes and their sorptive characteristics toward HOCs. *Separation and Purification Technology*, **63**, 156–162.